

Supplementary Information

Materials

Peptide synthesis and purification: Fluorenylmethyloxycarbonyl chloride (Fmoc)-protected amino acids were purchased from AAPPTec (Louisville, KY, USA) except for Fmoc-Lys(N₃)-OH, which was purchased from Chem-Impex (Wood Dale, IL, USA). Fmoc-Rink-amide 4-methylbenzhydrylamine (MBHA) resin, O-benzotriazole-N,N,N',N'-tetramethyluronium-hexafluoro-phosphate (HBTU), piperidine, and diisopropylethylamine (DIEA) were also purchased from AAPPTec. Diethyl ether (DEE), trifluoroacetic acid (TFA), acetonitrile (ACN), N,N-dimethylformamide (DMF), dichloromethane (DCM), and diisopropylcarboimide (DIC) were purchased from VWR (Radnor, PA, USA). Triisopropylsilane (TIS) and ethyl 2-cyano-2-(hydroxyamino)acetate (Oxyma) were purchased from MilliporeSigma (Burlington, MA, USA). Dithiothreitol (DTT) was purchased from AGTC bioproducts (Alachua, FL, USA). Ninhydrin test kit was purchased from Anaspec (Fremont, CA, USA).

Peptide-PCL conjugate synthesis: Anhydrous N-methyl pyrrolidine (NMP), dimethyl sulfoxide (DMSO), and deuterated dimethyl sulfoxide (DMSO-d₆) were purchased from VWR (Radnor, PA, USA). Poly(caprolactone) (PCL) (M_w 14,000 Da) and deuterated dichloromethane (CD₂Cl₂) were purchased from MilliporeSigma (Burlington, MA, USA). P-maleimidophenyl isocyanate (PMPI) was purchased from Chem-Impex.

Peptide-PCL inks: PCL (M_n 80,000 Da) was generously provided by Polysciences, Inc. (Warrington, PA, USA). 1,1,1,3,3,3,-Hexafluoro-2-propanol (HFIP) was purchased from Oakwood Chemical (Estill, SC, USA).

Peptide labeling: Phosphate buffered saline (PBS) tablets, dimethyl sulfoxide (DMSO), and isopropyl alcohol (IPA) were purchased from VWR. Bovine serum albumin (BSA), polyoxyethylenesorbitan monolaurate (TWEEN 20), streptavidin-conjugated fluorescein isothiocyanate (streptavidin-FITC), dibenzocyclooctyne-cyanine3 (DBCO-Cy3), Triton X-100, sodium azide, N-Hydroxysuccinimide (NHS), and 1-ethyl-3(3-dimethylaminopropyl)carbodiimide (EDC) were purchased from Sigma-Aldrich (St Louis, MO, USA). Hyaluronate fluorescein (fl-HA) (MW 50K) was purchased from Creative PEGWorks (Durham, NC, USA), Cyanine3 amine (amino-Cy3) from BroadPharm (San Diego, CA, USA), and Pierce™ 20X borate buffer from ThermoFisher Scientific (Waltham, MA, USA).

Cell culture and analysis: All cell culture reagents were purchased from ThermoFisher Scientific (Waltham, MA, USA) and all cell culture plasticware were from VWR, unless otherwise stated. Human mesenchymal stem cells (hMSCs) and RoosterNourish™-MSC media were purchased from Rooster Bio (Frederick, MD, USA). L-Ascorbic acid, bovine serum albumin (BSA), papain, sodium phosphate dibasic, ethylenediaminetetraacetic acid disodium salt dihydrate (EDTA), and N-acetyl cysteine were purchased from Sigma-Aldrich (St Louis, MO, USA). Trypsin ethylenediaminetetraacetic acid (Trypsin-EDTA) and antibiotic/antimycotic were purchased from Corning (Corning, NY, USA). Sylgard™ 184 Silicone Elastomer and calf thymus DNA (CT-DNA) was purchased from VWR. Paraformaldehyde (PFA) was purchased from Alfa Aesar (Haverhill, MA, USA). Hoescht 33258 and 1,9-Dimethyl-Methylene Blue zinc chloride double were purchased from MilliporeSigma (Burlington, MA, USA). Quant-iT™ Picogreen® dsDNA Assay Kit was purchased from ThermoFisher Scientific (Waltham, MA, USA).

Tissue staining: Sucrose, Tissue-Tek® O.C.T. Compound, acetic acid, and Alizarin Red S sodium salt were purchased from VWR (USA). Alcian Blue 8GX powder was purchased from ThermoFisher Scientific (Waltham, MA, USA). Nuclear Fast Red was purchased from Sigma-Aldrich (St Louis, MO, USA). Proteinase K was purchased from Agilent Technologies (Santa Clara, CA, USA). Normal goat serum (NGS) was purchased from Abcam (Cambridge, UK).

Peptide Synthesis and Purification

Peptides were synthesized and purified as previously described.^{1,2} Peptides were synthesized on MBHA resin (100-200 mesh, 0.67 mmol/g functionalization) using standard Fmoc solid-phase peptide synthesis (SPPS), either manually or using a CEM Liberty Blue automated microwave peptide synthesizer (CEM Corporation, Matthews, NC, USA).

Manual SPPS

Manual SPPS was performed at 0.5 or 1 mM scale using 100 mL peptide synthesis vessels (Chemglass) and a wrist-action shaker (Burrell). For each coupling, the Fmoc protecting group was removed with 20% piperidine in DMF followed by washing with DCM and DMF. Amino acids were activated by adding 3.95 molar equivalents of HBTU to 4 molar equivalents of the Fmoc-protected amino acids in DMF. DIEA was added at 6 molar equivalents to the amino acid solution before adding the coupling solution to the resin. The reaction was allowed to proceed for 2 hours before washing the resin thoroughly with DCM and DMF. Ninhydrin tests (Cambridge

Biosciences) were performed after each Fmoc deprotection and coupling reaction to monitor the presence of free amines. For the HAbind(biotin) peptide, an Fmoc-Lys(Mtt)-OH was coupled manually and biotinylated (see *Biotinylation of HAbind(biotin)*), and the remaining amino acids were coupled using the synthesizer.

Biotinylation of HAbind(biotin)

Fmoc-Lys(Mtt)-OH was manually coupled to the MBHA resin using methods described above. The Mtt protecting group was removed using 5% TFA solution in DCM. The ϵ -amine on the lysine side chain was biotinylated using a 2-fold excess of biotin/HBTU dissolved in a 50:50 DMSO:DMF solution with 3 molar excess of DIEA, and allowed to couple overnight. Coupling was repeated with a new solution for 2 hours before verifying coupling using a ninhydrin test at room temperature. The resin was transferred to the microwave peptide synthesizer to couple the remaining amino acids.

Automated SPPS

Peptides synthesized on the automated microwave peptide synthesizer were prepared at a 0.5 or 1 mM scale using standard methods developed by CEM. Coupling reactions were activated using 10 molar equivalents each of DIC and Oxyma.

Peptides were cleaved from the resin in a solution of 95% TFA, 2.5% TIS, 2.5% ultrapure water, and 2.5% DTT for 4 hours. TFA was removed using rotary evaporation, and the peptide was precipitated in cold DEE. The precipitate was collected using centrifugation and allowed to dry overnight under vacuum.

Purification

Crude peptides were dissolved in acidic mobile phase (5% ACN in ultrapure water with 0.1% TFA), sonicated until fully solubilized, and passed through a 0.45 μ m filter before purification. Peptides were purified using reversed-phase preparative high-performance liquid chromatography (HPLC; Agilent 218 Prep HPLC, Agilent Technologies, Santa Clara, CA, USA) with a mobile phase gradient of 5% ACN and 95% ultrapure water to 100% ACN with 0.1% TFA on an Agilent 5 Prep-C18 column (150 x 21.2 mm, 5 μ m pore size, 100 Å particle size). Fractions were collected separately, rotary evaporated to remove excess ACN, and lyophilized using a Labconco Freezone freeze dryer (Labconco, Kansas City, MO, USA). The masses for each purified peptide were verified using matrix-assisted laser ionization (MALDI; Shimadzu 8020,

Kyoto, Japan), electrospray ionization mass spectrometry (ESI-MS; Applied Biosystems 3200 Q Trap, Foster City, CA, USA; or Thermo Fisher LTQ-XL™, Waltham, MA, USA). The purified peptides were also evaluated by HPLC with an Agilent 5 Prep-C18 analytical column (150 x 4.6 mm, 5 μm pore size, 100 Å particle size). Mass spectrometry and analytical HPLC spectra for each purified peptide are shown in Figures S1-S4.

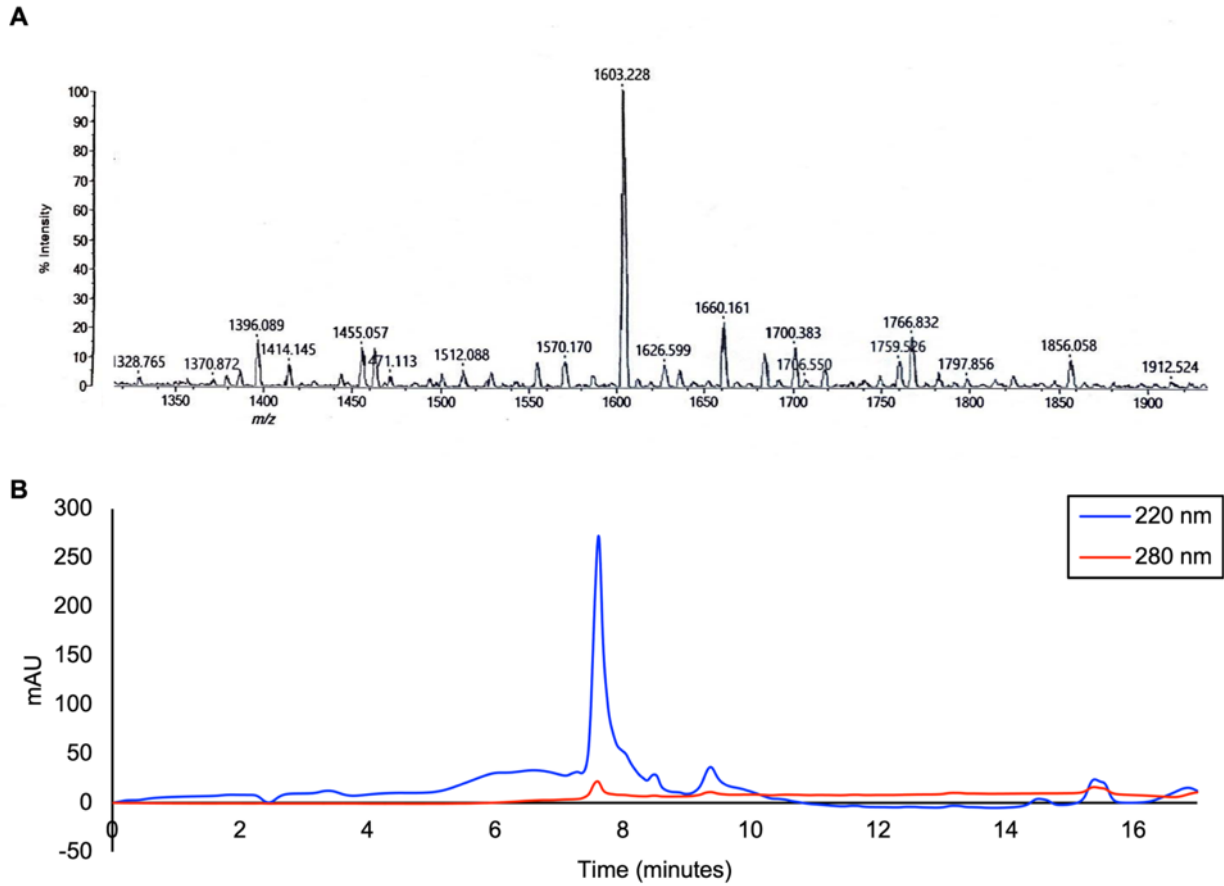


Figure S1. (A) MALDI and (B) analytical HPLC of the purified HABind peptide CGGGRYPIISRPRKR (MW 1602 g/mol).

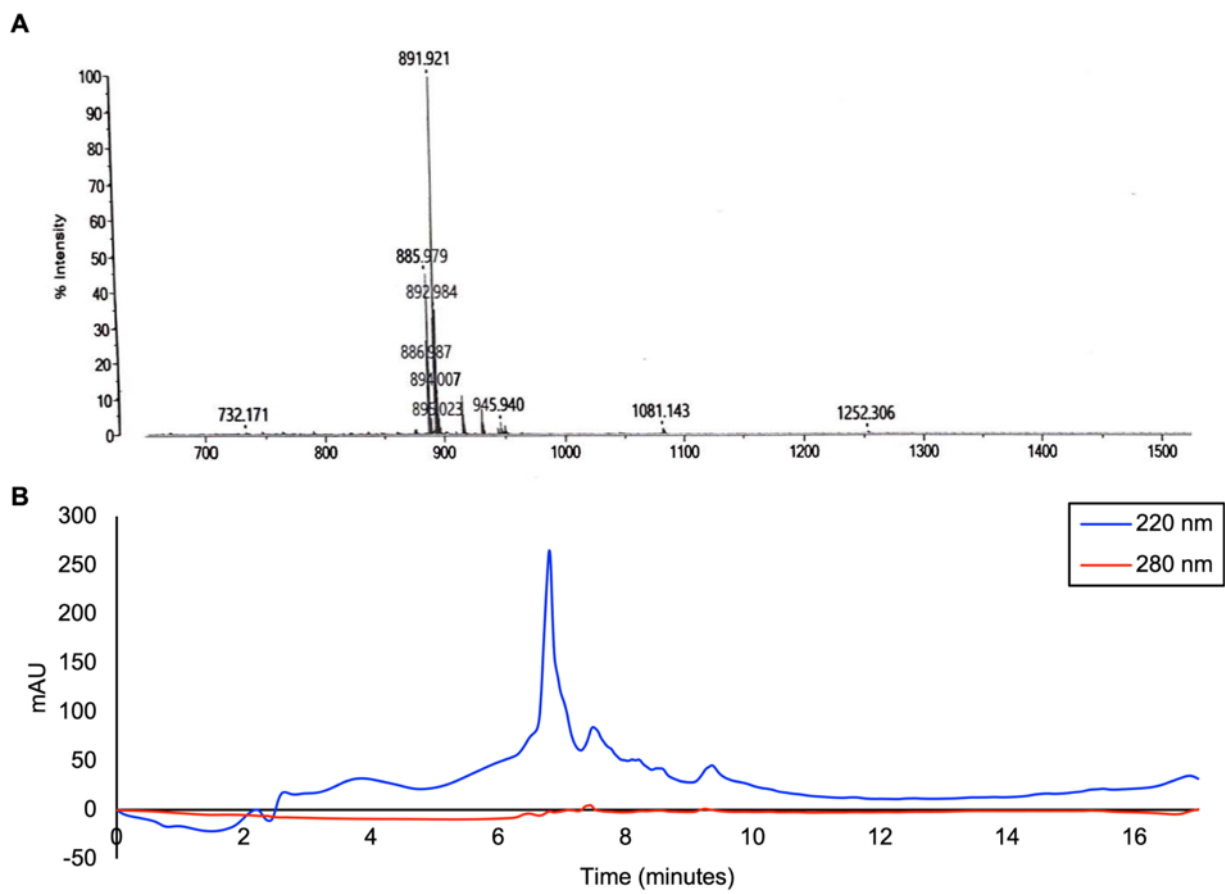


Figure S2. (A) MALDI and (B) analytical HPLC of the purified E3 peptide CGGGAAEEE (MW 892 g/mol).

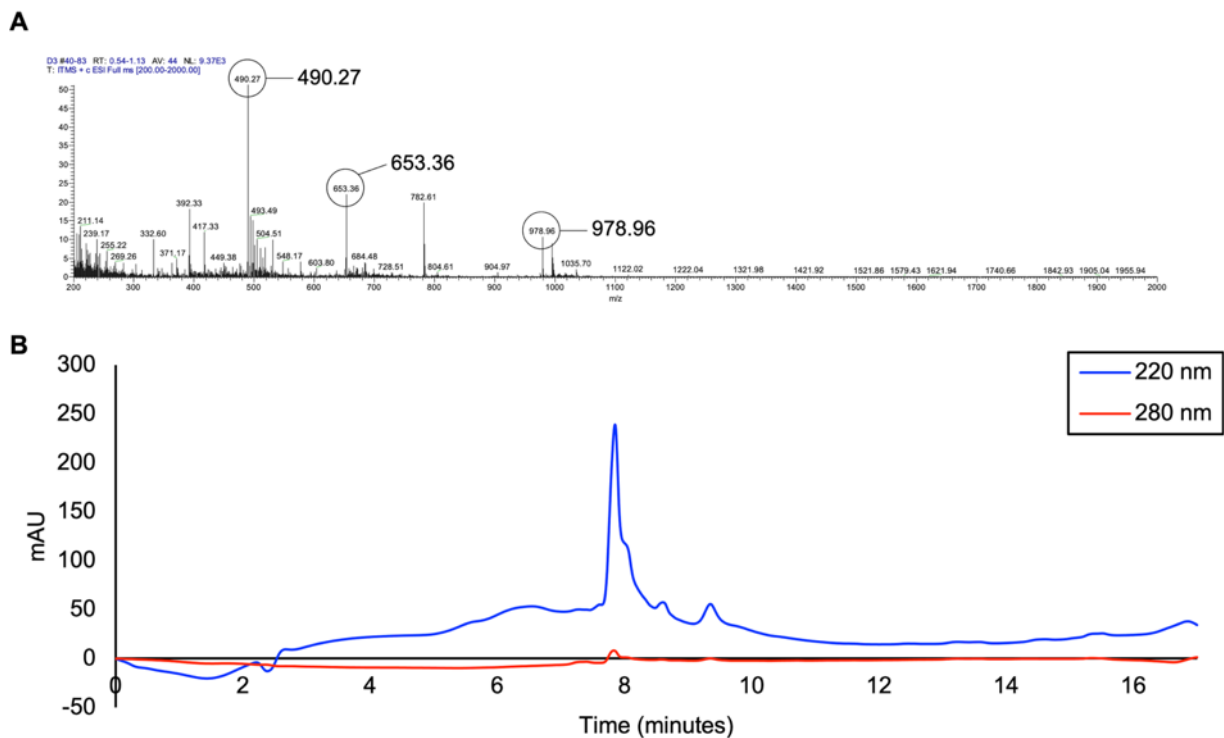


Figure S3. (A) ESI-MS of purified HABind(biotin) CGGGYPISRPRKRK(biotin) (MW 1956 g/mol) showing $[M/2 + H]$, $[M/3 + H]$, and $[M/4 + H]$ ions and (B) corresponding analytical HPLC.

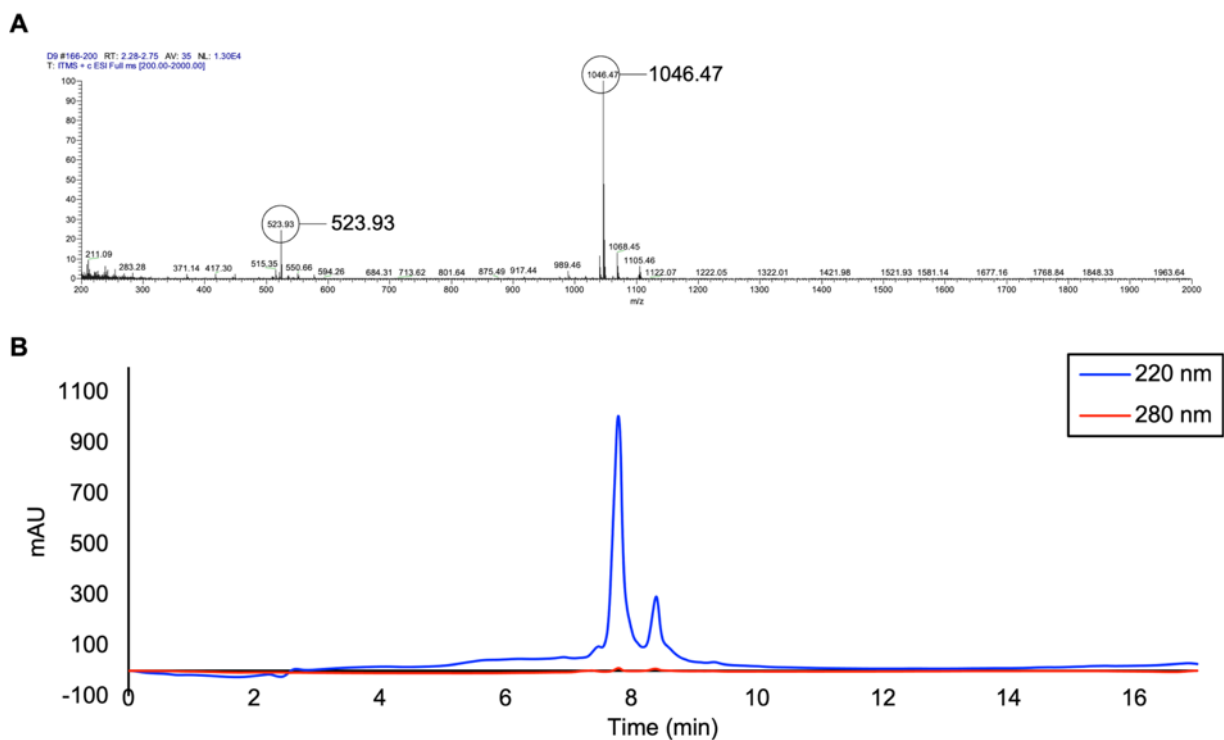


Figure S4. (A) ESI-MS of purified E3(azide) CGGGAAEEEEK(azide) (MW 1046 g/mol) showing $[M/2 + H]$ ion and (B) corresponding analytical HPLC.

Peptide-PCL conjugate synthesis

Conjugates were synthesized using methods similar to published methods.^{1,2} Each synthesis step was confirmed by ¹H NMR using a Bruker Biospin Advance III HD 400 MHz NMR spectrometer or a Bruker Neo 500 MHz NMR spectrometer. PCL (M_w 14,000, M_n 10,000) was dissolved at 80-100 mg/mL in anhydrous NMP under nitrogen. PMPI at 15-20 fold molar excess to PCL was separately dissolved in anhydrous NMP and added dropwise to the PCL solution while stirring under nitrogen. The reaction was allowed to react overnight. The resulting PCL-maleimide (PCL-mal) product was precipitated into diethyl ether (DEE) to remove excess PMPI. PMPI and PCL-mal were dissolved in CD₂Cl₂. Proton assignments of the PMPI and PCL-maleimide were based on published spectra.²⁻⁴ ¹H-NMR showed that PMPI was successfully conjugated to PCL to form PCL-mal (**Fig. S5**).

To conjugate the peptide, PCL-mal was re-dissolved in anhydrous NMP under nitrogen. The peptides were separately dissolved in dimethyl sulfoxide (DMSO) (E3 and E3(azide)) or anhydrous NMP (HAbind and HAbind(biotin)) at 8 molar equivalents before adding dropwise to the PCL-mal solution while stirring under nitrogen. The reaction was continued overnight. The resulting peptide-PCL conjugates were precipitated in DEE, washed with ultrapure water to remove excess peptide, and dried under vacuum prior to analysis. All peptides and peptide-PCL conjugates were dissolved in DMSO-d₆ or DMF-d₇. ¹H-NMR showed that peptides were successfully conjugated to PCL-mal to form the respective peptide-PCL conjugates (**Fig. S6-S9**).

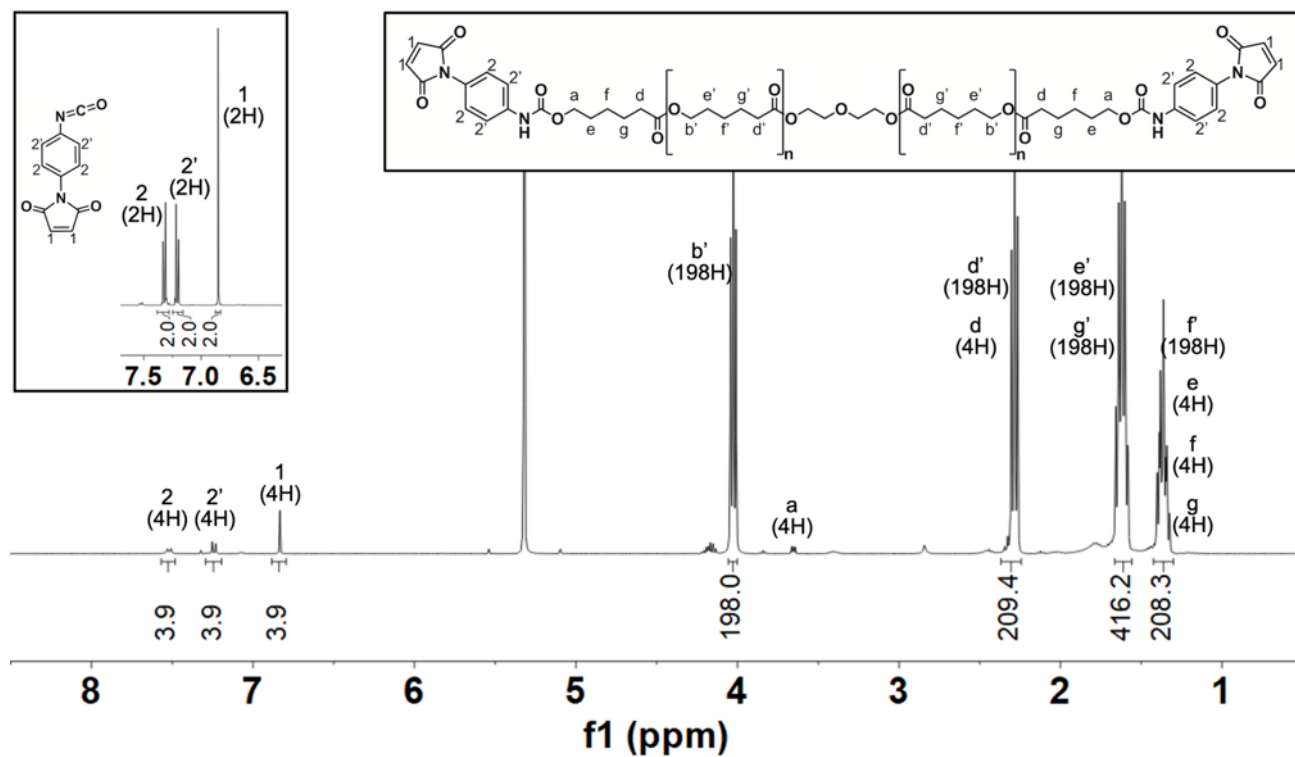


Fig S5. Representative ¹H NMR (400MHz, CD₂Cl₂, TMS) and corresponding chemical structures of p-maleimidophenyl isocyanate (PMPI; inset) with chemical shift assignments 6.85 (2H, s, maleimide vinyl, 1), 7.21 (2H, d, Ar-H ortho to isocyanate, 2'), 7.32 (2H, d, Ar-H ortho to maleimide, 2) and PCL-maleimide with chemical shift assignments 6.83 (4H, s, maleimide vinyl, 1), 7.24 (4H, d, Ar-H ortho to isocyanate, 2'), 7.52 (4H, d, Ar-H ortho to maleimide, 2), 4.03 (198H, m, -O-CH₂-, b'), 3.65 (4H, m, -O-CH₂-, a), 2.28 (205H, m, -CO-CH₂-, d, d'), 1.62 (440H, m, -CH₂-, e, g'), 1.36 (207H, m, -CH₂-, f, e, f, g).

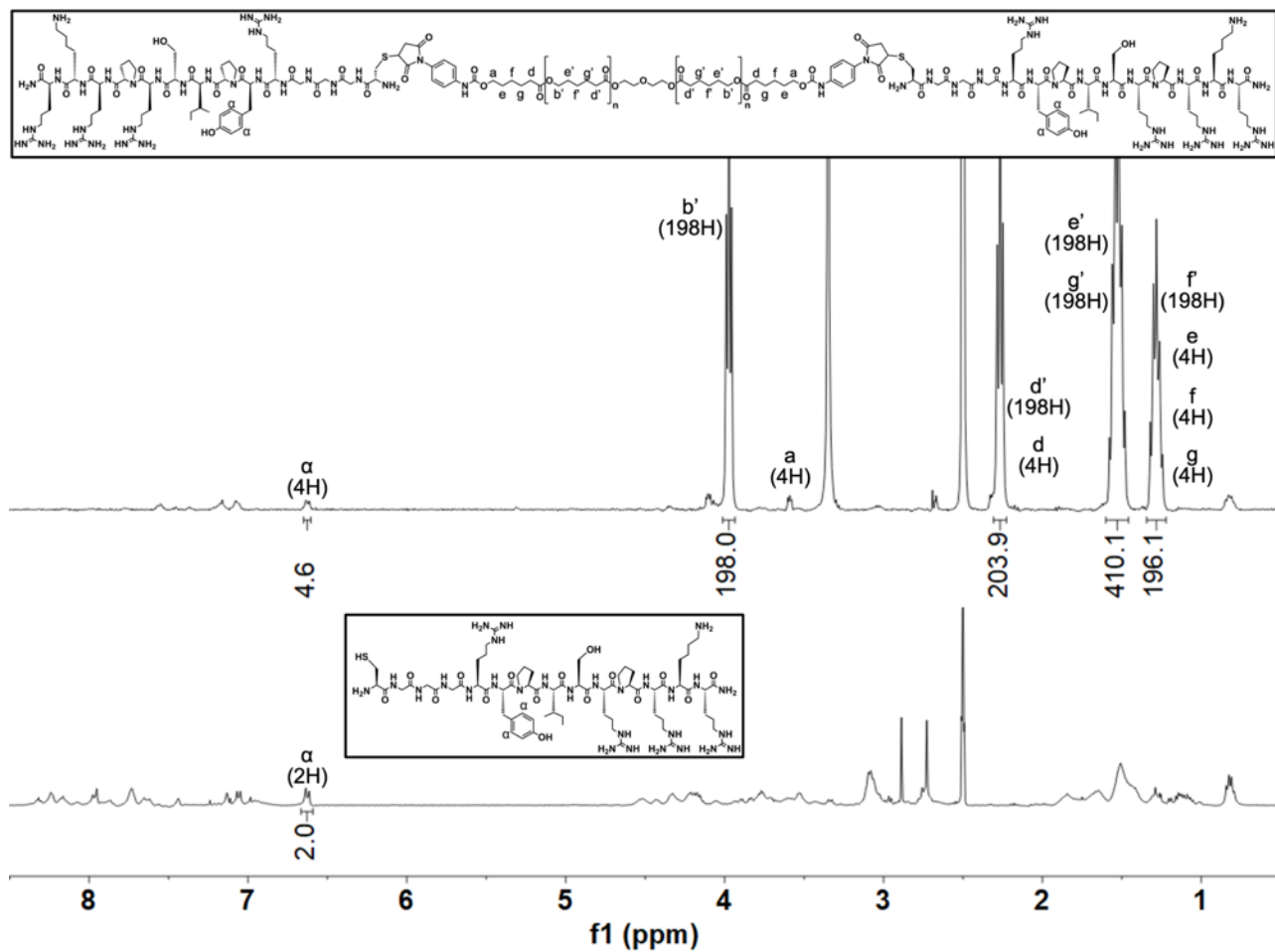


Figure S6. ¹H NMR (400MHz, DMSO-d₆, TMS) and corresponding chemical structures of HABind-PCL (top) with chemical shift assignments 6.62 (4H, d, Ar-H, a), 3.97 (198H, m, -O-CH₂-, b'), 3.60 (4H, m, -O-CH₂-, a), 2.27 (207H, m, -CO-CH₂-, d, d'), 1.53 (436H, m, -CH₂-, e, g'), 1.28 (215H, m, -CH₂-, f, e, f, g) and HABind (bottom) with chemical shift assignment 6.62 (2H, m, Ar-H, a).

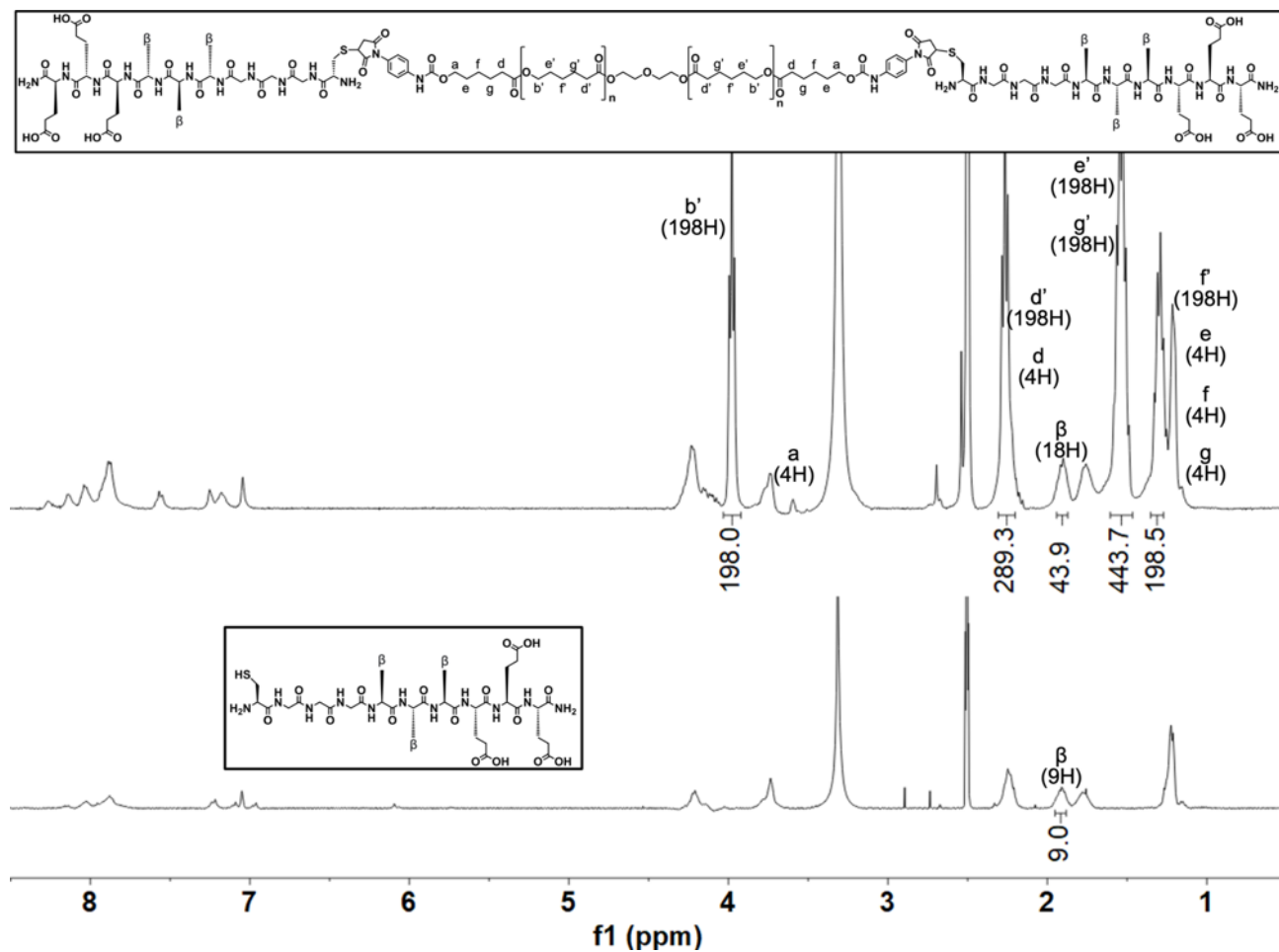


Figure S7. ^1H NMR (400MHz, DMSO-d_6 , TMS) and corresponding chemical structures of E3-PCL (top) with chemical shift assignments 3.98 (198H, m, $-\text{O}-\text{CH}_2-$, b'), 3.60 (4H, m, $-\text{O}-\text{CH}_2-$, a), 2.27 (210H, m, $-\text{CO}-\text{CH}_2-$, d, d'), 1.91 (18H, m, $-\text{CH}_3$, β), 1.54 (421H, m, $-\text{CH}_2-$, e, g'), 1.30 (209H, m, $-\text{CH}_2-$, f, e, f, g) and E3 (bottom) with chemical shift assignment 1.91 (9H, m, $-\text{CH}_3$, β).

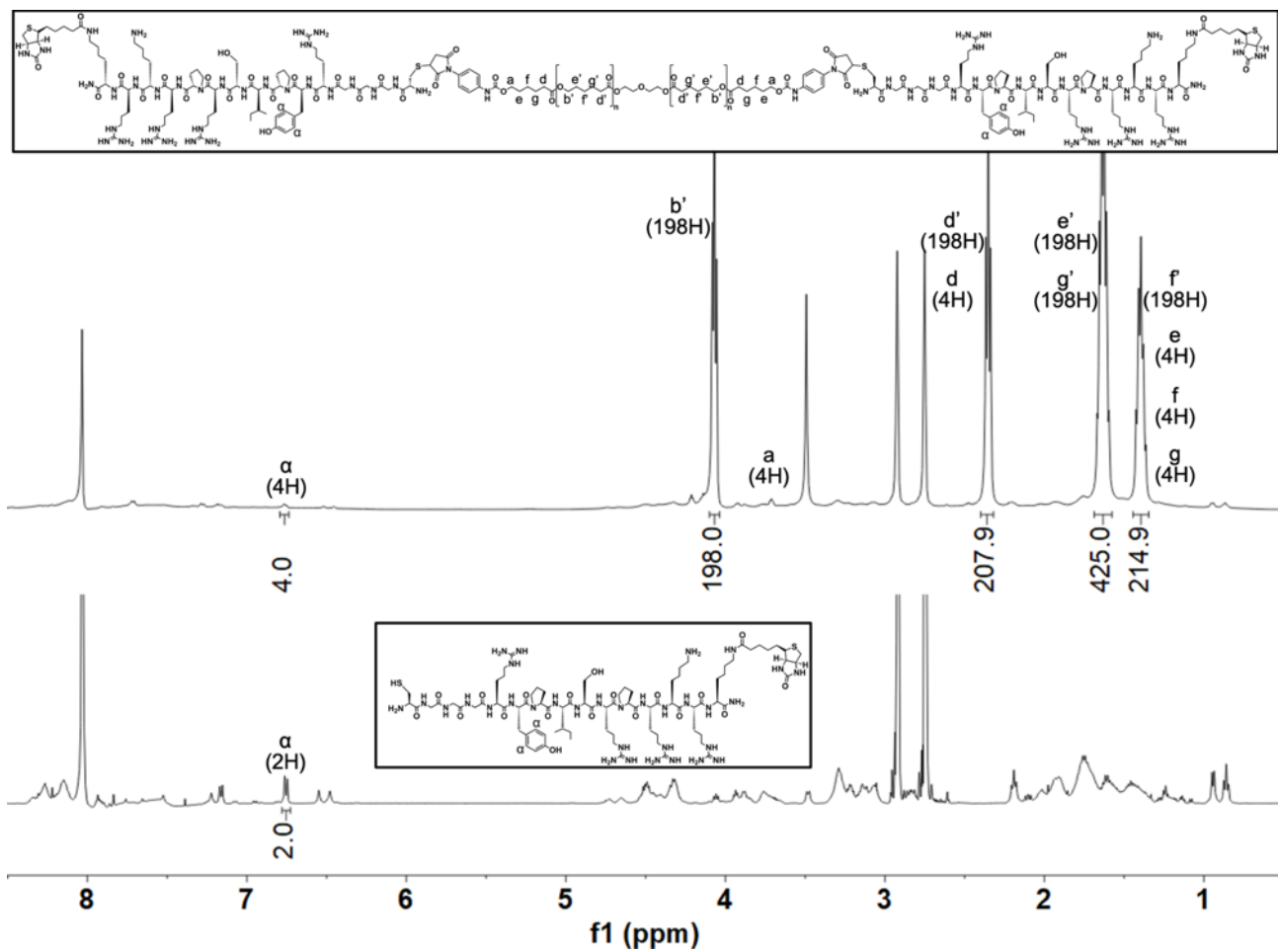


Figure S8. ¹H NMR (500MHz, DMF-d₇, TMS) and corresponding chemical structures of HABind(biotin)-PCL (top) with chemical shift assignments 6.75 (4H, d, Ar-H, a), 4.07 (198H, m, -O-CH₂-, b'), 3.60 (4H, m, -O-CH₂-, a), 2.35 (207H, m, -CO-CH₂-, d, d'), 1.64 (436H, m, -CH₂-, e, g'), 1.39 (215H, m, -CH₂-, f, e, f, g) and HABind(biotin) (bottom) with chemical shift assignment 6.75 (2H, m, Ar-H, a).

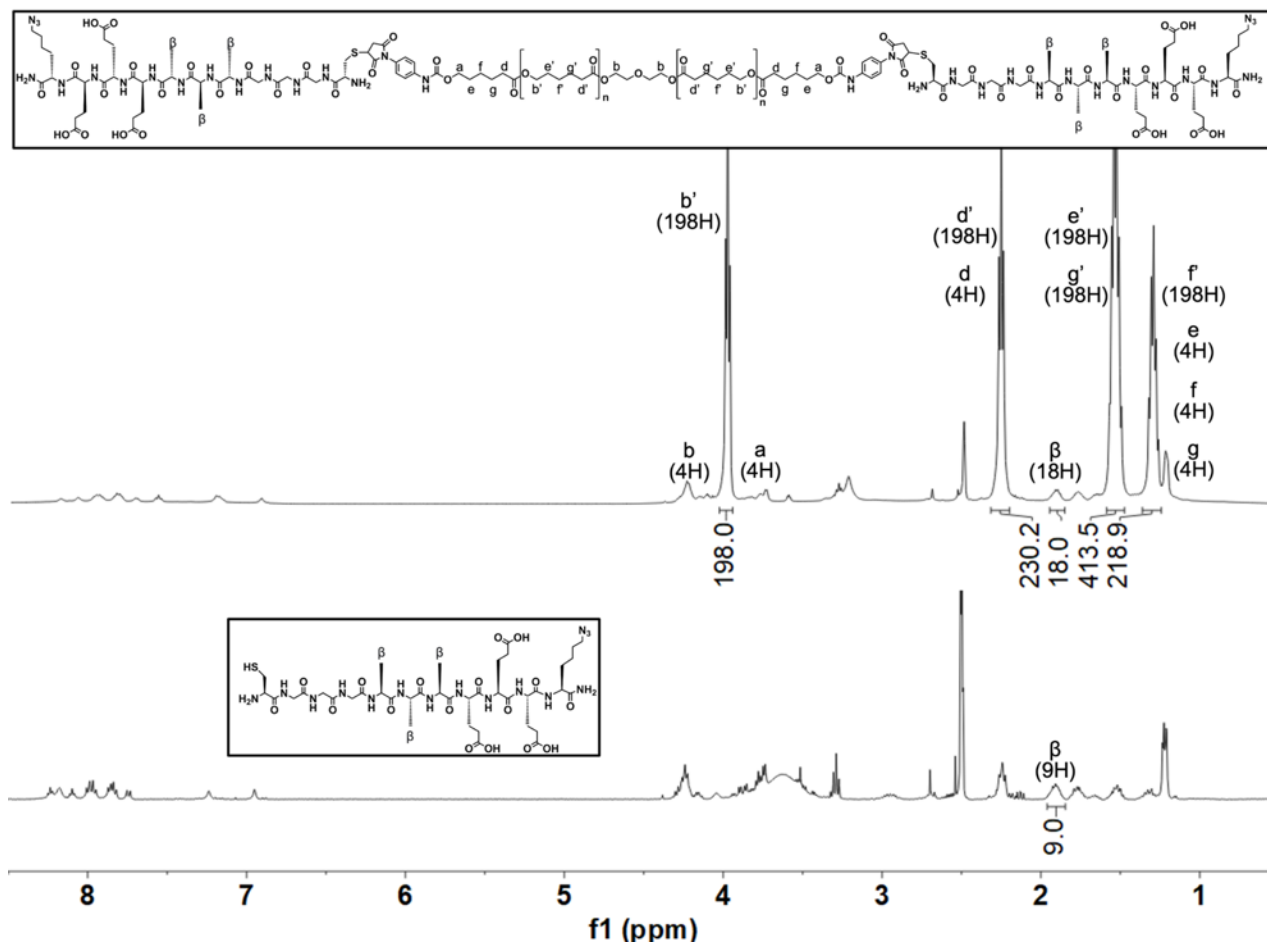


Figure S9. ¹H NMR (500MHz, DMSO-d₆, TMS) and corresponding chemical structures of E3(azide)-PCL (top) with chemical shift assignments 3.99 (198H, m, -O-CH₂-, b'), 3.60 (4H, m, -O-CH₂-, a), 2.27 (210H, m, -CO-CH₂-, d, d'), 1.91 (18H, m, -CH₃, β), 1.55 (421H, m, -CH₂-, e, g'), 1.31 (209H, m, -CH₂-, f', e, f, g) and E3(azide) (bottom) with chemical shift assignment 1.91 (9H, m, -CH₃, β).

3D-printed peptide-functionalized scaffolds

Samples were mounted on 12-mm aluminum stubs using carbon tape, then sputter-coated with iridium using a sputter coater (Electron Microscopy Sciences EMS575X, Hatfield, PA, USA). Samples were imaged with a scanning electron microscope (SEM) (LEO 1550 SEM; Zeiss, Peabody, MA, USA) using a secondary electron detector with an accelerating voltage of 5 kV.

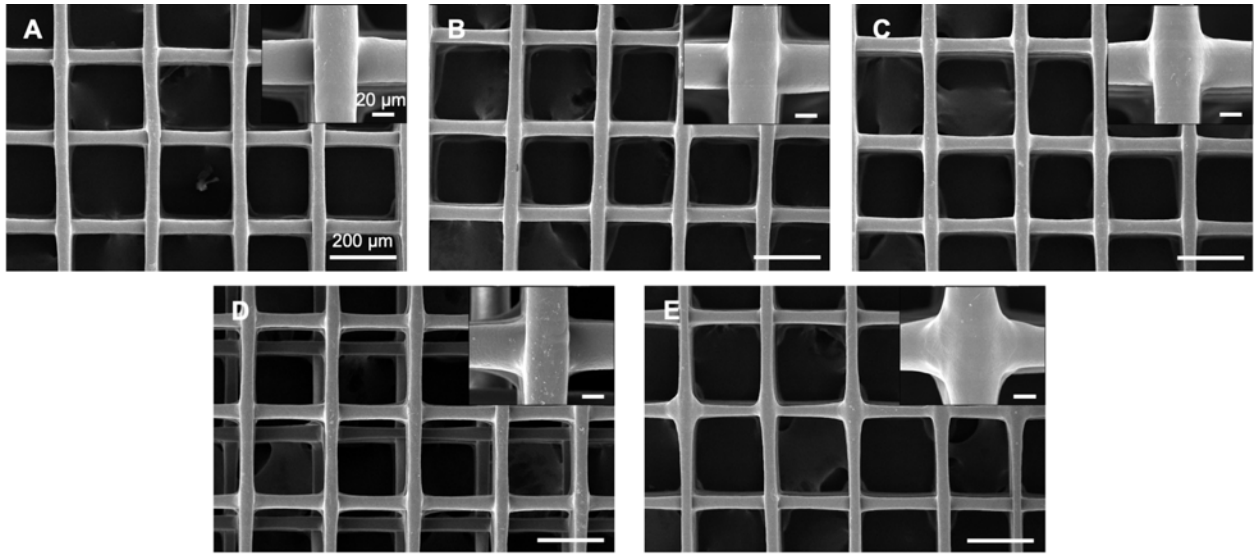


Figure S10. Representative scanning electron microscopy (SEM) images of scaffolds 3D-printed with inks containing (A) PCL only, (B) 18 mg/mL E3-PCL, (C) 3 mg/mL HABind-PCL, (D) 18 mg/mL E3-PCL or HABind-PCL printed in opposing zones (dual spatial), or (E) 18 mg/mL E3-PCL and HABind-PCL homogeneously mixed (dual mixed), with higher magnification shown in the inset. These images demonstrated that scaffold morphology and topography was unaffected by addition of the conjugates.

Peptide presentation during culture

PCL, HABind-PCL, and E3-PCL scaffolds were sterilized in 70% v/v ethanol for 30 minutes, washed with sterile water, incubated in sterile 0.1% w/v BSA for at least 4 hours, and rinsed thoroughly with sterile water. Scaffolds were incubated in growth media (DMEM-GlutaMAX™ supplemented with 10% v/v FBS, 1% v/v anti/anti, and 50 μg/mL ascorbic acid) for 60 days at 37°C and 5% CO₂. Media was changed every 2-3 days to replicate cell culture conditions. Samples from each group were harvested after sterilization and after culture.

Scaffolds were labeled using amino-Cy3 to tag carboxyl groups present in the E3 peptide^{4,5} or fluorescently tagged hyaluronic acid (fl-HA) to confirm binding to the hyaluronic acid (HA)-binding sequence^{3,4}. To label with amino-Cy3, PCL and E3-PCL scaffolds were blocked with 0.2% v/v TWEEN 20 and 0.2% v/v Triton X-100 in PBS (block solution C) for 60 minutes and washed with ultrapure water. After blocking, scaffolds were incubated at room temperature in 0.1 mM amino-Cy3 in 20 mM sodium borate buffer combined with 0.2 mM 1-ethyl-3(3-dimethylaminopropyl)carbodiimide (EDC) and 0.2 mM N-hydroxysuccinimide (NHS) for 30 minutes then washed with 20 mM sodium borate buffer, ultrapure water, block solution C, ultrapure water, 50% v/v IPA, 100% v/v IPA, 50% v/v IPA, and ultrapure water for 10 minutes each. To label with fl-HA, PCL and HABind-PCL scaffolds were blocked in 0.5% w/v BSA overnight and washed twice with PBS for 30 minutes each. After blocking, scaffolds were incubated for 60 minutes in 0.1 mg/mL fl-HA solution in PBS then washed with PBS three times and ultrapure water for 30 minutes each. Fluorescence intensity was read on a Tecan Infinite M200 Pro plate reader (Männedorf, Switzerland). One-way ANOVA with simple contrasts was performed to compare between specific groups. Differences were considered significant for p-values < 0.05.

Fluorescence quantification demonstrated that the peptides were still available on the surface of peptide-functionalized scaffolds after 2 months in culture (**Fig. S11**). Fluorescence intensity was higher in E3-PCL scaffolds compared to PCL controls, both before (p=0.034) and after 2 months in culture (p=0.002) (**Fig. S11A**). Furthermore, fluorescence intensity of E3-PCL scaffolds was not significantly different after 2 months in culture (p=0.49). HABind-PCL scaffolds after 2 months in culture showed lower fluorescence intensity compared to before culture (p=0.037). Protein absorption on the scaffold surface during culture likely affected the interaction between the HABind peptides and the larger molecular size fl-HA polymers. However, HABind-PCL scaffolds showed higher fluorescence intensity at 0 months (p<0.001) and 2 months of culture (p=0.011) compared to PCL controls (**Fig. S11B**). Together, fluorescent labeling demonstrated E3 and HABind peptides were displayed on the fiber surface and the sequences were available up to 2 months in culture.

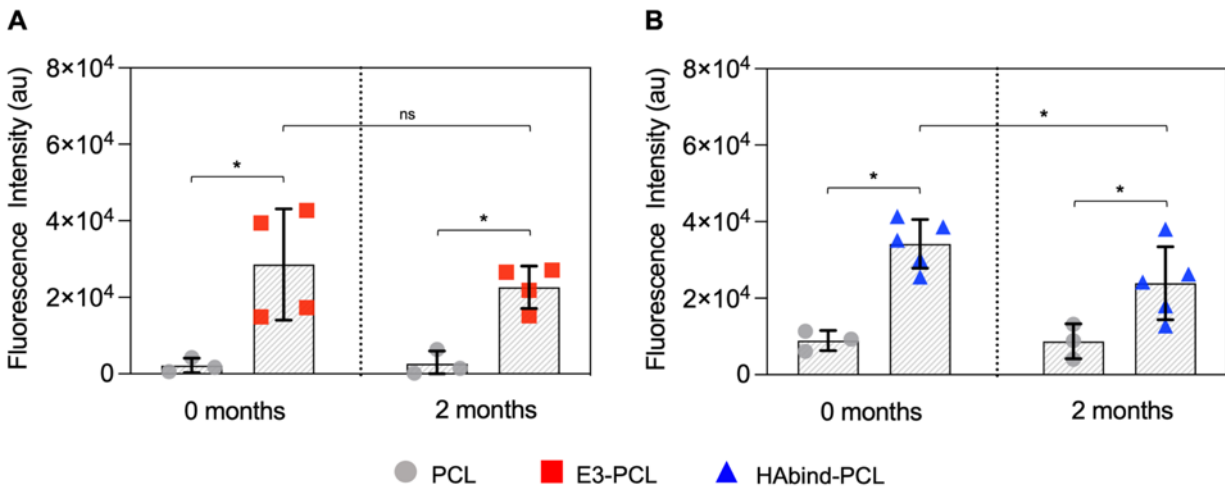


Fig S11. Fluorescence intensity quantification of (A) E3-PCL and control PCL scaffolds labeled with amino-Cy3 and (B) HABind-PCL and control PCL scaffolds labeled with fluorescein-HA, before and after 2 months in culture (n=3-5 scaffolds per group). Data presented as mean \pm SD (significance * $p < 0.05$).

Cell response to 3D-printed scaffolds with increasing peptide concentration

We investigated if peptide concentration influenced hMSC behavior by comparing scaffolds printed with different concentrations of HABind-PCL (1, 3, 6 mg/mL) or E3-PCL (6, 12, 18 mg/mL) to PCL only controls. Upregulation of *SOX9* was observed at Day 14 in 12 mg/ml E3-PCL, 1 mg/ml HABind-PCL, and 6 mg/ml HABind-PCL scaffolds ($p=0.082$, $p=0.022$, and $p=0.087$, respectively) (**Fig. S12A**). Higher glycosaminoglycan (GAG) accumulation was only observed at Day 7 in 6 mg/ml E3-PCL and 12 mg/ml E3-PCL compared to PCL ($p=0.09$ and $p=0.026$, respectively) (**Fig. S12A**). All concentrations of HABind-PCL upregulated *RUNX2* expression at Day 14 compared to PCL ($p=0.029$, $p=0.021$, and $p=0.03$, for HABind-PCL 1, 3, and 6 mg/ml respectively) (**Fig. S12B**). The 6 mg/mL HABind-PCL showed lower ALP activity compared to PCL ($p=0.093$) (**Fig. S12B**). Despite significant differences in chondrogenic and osteogenic markers at specific timepoints, no overall trend indicated an optimal concentration for single peptide scaffolds that drove differentiation.

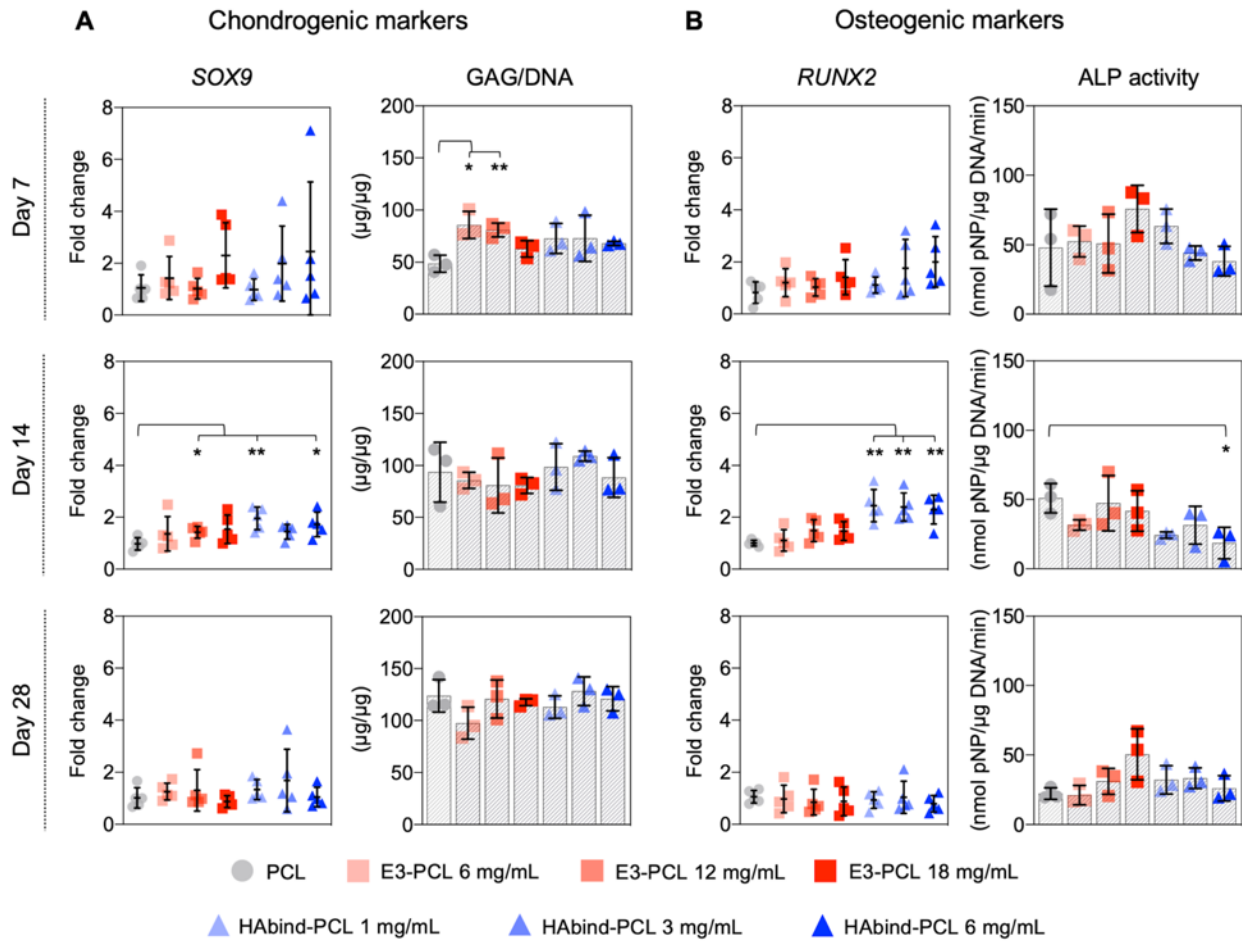


Figure S12. (A) Chondrogenic and (B) osteogenic markers measured in single-peptide constructs with different conjugate concentrations cultured for up to 28 days without added differentiation factors. *SOX9* and *RUNX2* gene expression was measured by RT-qPCR, normalized to 18S, and reported as fold-difference relative to PCL at each time point (n=5). Biochemical analysis of GAG content was normalized to DNA. ALP activity was normalized to DNA and time of reaction (n=3). Data presented as mean \pm SD (significance *p<0.1, **p<0.05).

Cell response to single or dual-peptide presentation on 3D-printed scaffolds

Cell proliferation was evaluated after 14 and 28 days in culture by DNA quantification. No significant differences in DNA content were observed among scaffold groups (**Fig. S13**)

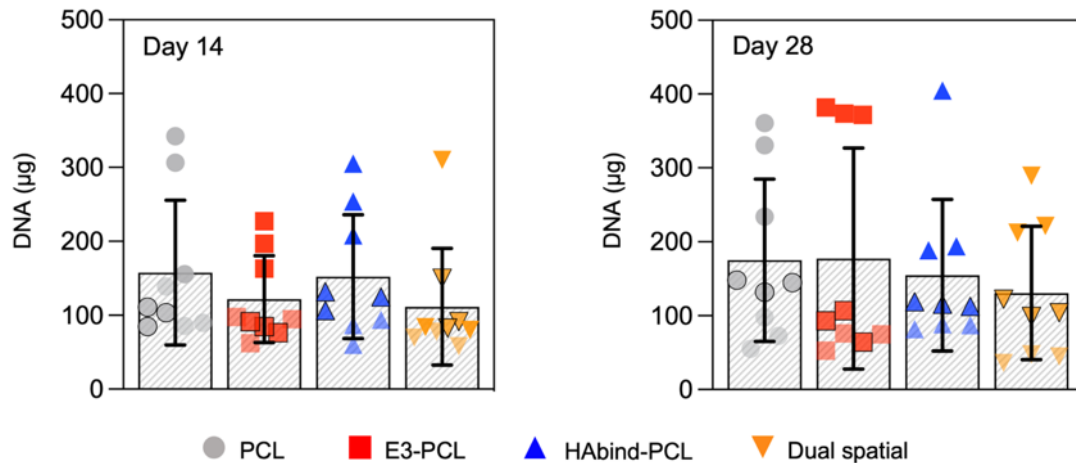


Figure S13. DNA content measured in PCL, E3-PCL, HABind-PCL, and dual spatial constructs cultured for 14 and 28 days (left to right). Data from three independent experiments with different donors represented in different shades (light = Donor A; medium with black border = Donor B; dark = Donor C) (3 scaffolds per donor in each scaffold group; n=9 scaffold total per group). Data is presented as mean \pm SD (significance * $p < 0.1$, ** $p < 0.05$).

GAG deposition and calcium accumulation were evaluated after 28 days in culture by histological staining with Alcian blue and Alizarin Red, respectively. Alcian blue staining showed higher GAG accumulation in dual spatial and E3-PCL scaffolds compared to PCL and HABind-PCL (**Fig. S14**). This was observed as more intense blue staining in histological sections the scaffolds. All scaffolds presented similar Alizarin Red staining, suggesting no differences in calcium deposition between groups. No intense orange-red staining was observed in the constructs, indicating little to no calcium deposition in the scaffolds at this timepoint.

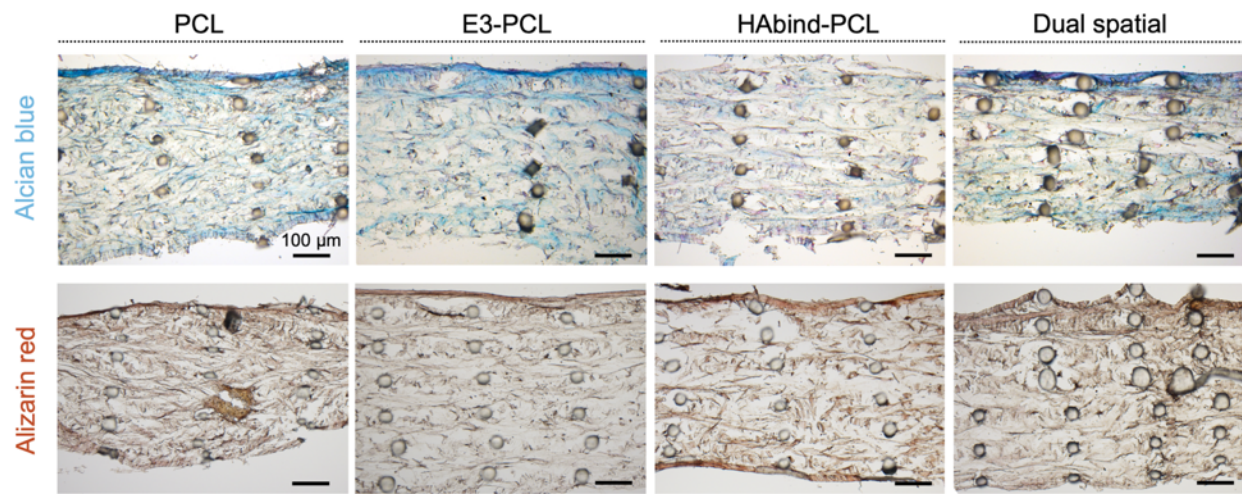


Figure S14. Representative microscopy images of histological cross-sections showing Alcian blue (top) and Alizarin Red staining (bottom) in PCL, E3-PCL, HAbind-PCL, and dual spatial scaffolds (L to R). Dual spatial and E3-PCL scaffolds showed higher GAG accumulation than PCL and HAbind-PCL scaffolds, demonstrated by more intense blue staining. Scaffolds showed no measurable calcium accumulation, as shown by the absence of intense orange-red staining. (Scale bar = 100 μm)

Cell response to multi-peptide spatial organization in 3D-printed scaffolds

Human MSC response to multi-peptide organization in 3D-printed scaffolds was evaluated with a gene expression profile containing chondrogenic and osteogenic markers (**Fig. S15**). Three independent donors were used in separate experiments to investigate scaffold effects across multiple donors.

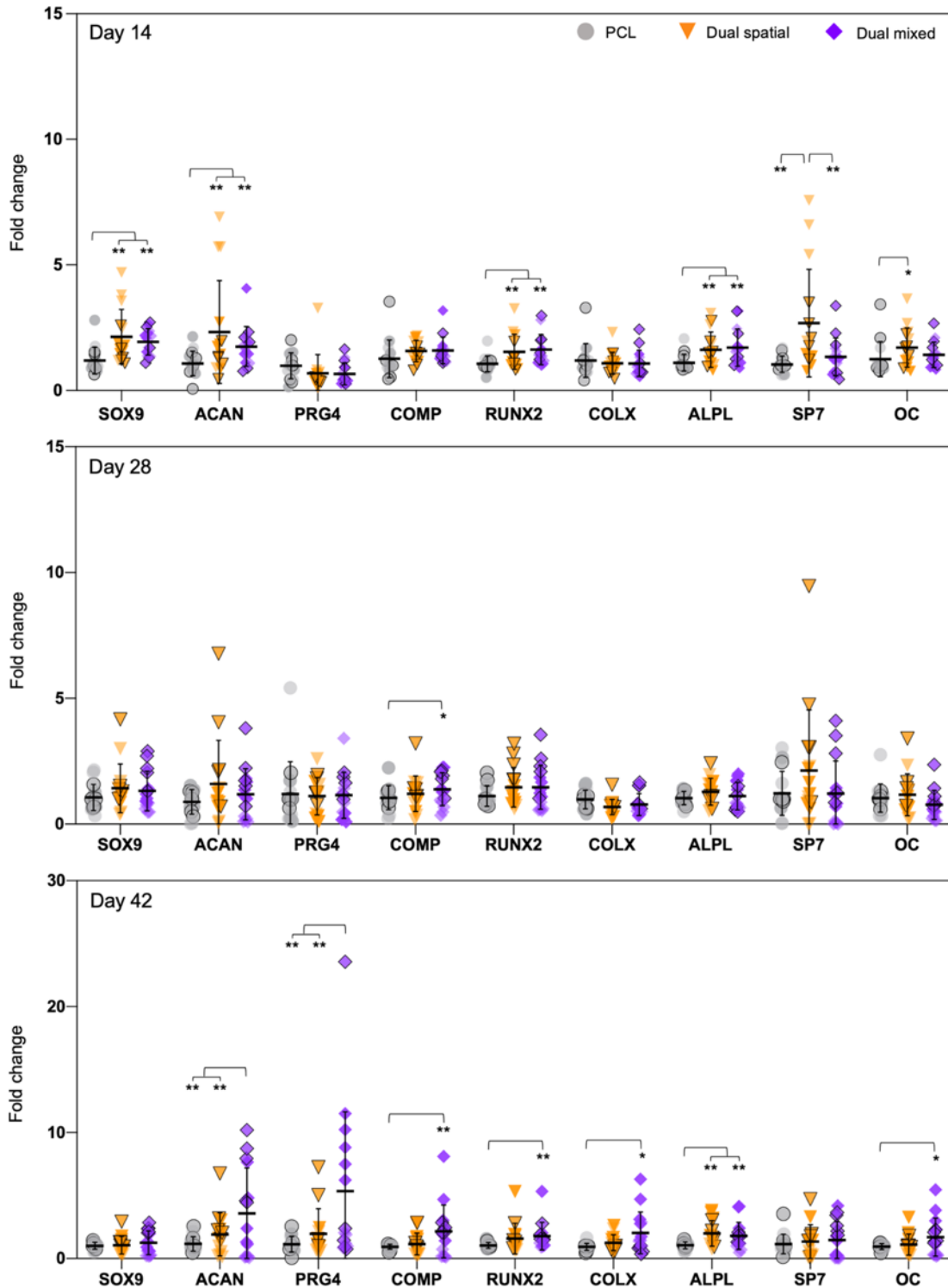


Figure S15. Gene expression measured in dual-peptide constructs cultured for 14, 28, and 42 days (top to bottom) without added differentiation factors. Data from three independent experiments with different donors represented in different shades (light = Donor B; medium with black border = Donor C; dark = Donor D). Gene expression was measured by RT-qPCR, normalized to 18S, and reported as fold-difference relative to PCL at each time point (4-5 scaffolds per donor in each scaffold group; n=14-15 scaffolds total per group). Data is presented as mean \pm SD (significance * p <0.1, ** p <0.05).

Cell proliferation was evaluated after 14, 28, and 34 days in culture by DNA quantification. No significant differences in DNA content were observed among scaffold groups (**Fig. S16**)

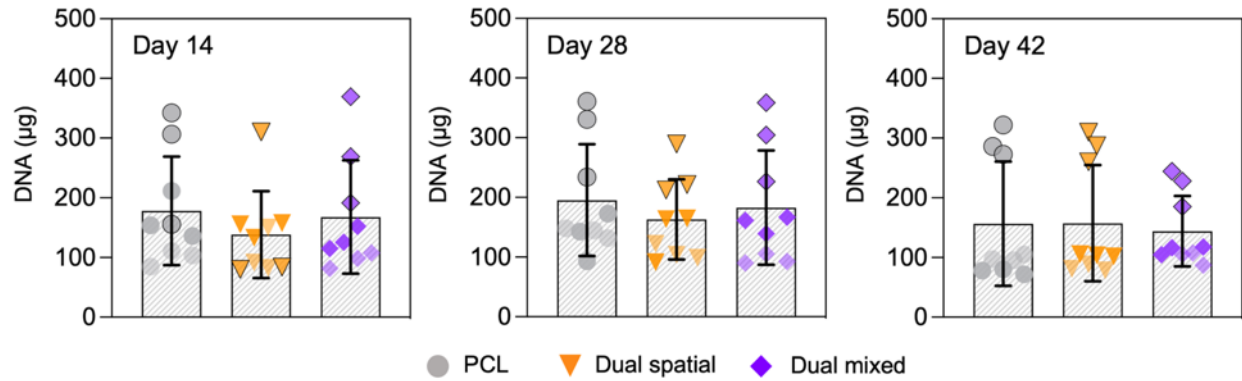


Figure S16. DNA content measured in PCL and multi-peptide constructs cultured for 14, 28, and 42 days (left to right). Data from three independent experiments with different donors represented in different shades (light = Donor B; medium with black border = Donor C; dark = Donor D) (3 scaffolds per donor in each scaffold group; n=9 scaffold total per group). Data is presented as mean \pm SD (significance * $p < 0.1$, ** $p < 0.05$).

GAG deposition and calcium accumulation were evaluated after 42 days in culture using Alcian blue and Alizarin Red staining, respectively. All scaffolds presented similar Alcian blue staining, suggesting no measurable differences in GAG accumulation between groups (**Fig. S17**). Alizarin Red staining showed some calcium deposits in dual spatial scaffolds, characterized by accumulation of intense orange-red dye (arrows in **Fig. S17**). The intense orange-red staining was not observed in PCL or dual mixed scaffolds, suggesting minimal calcium accumulation.

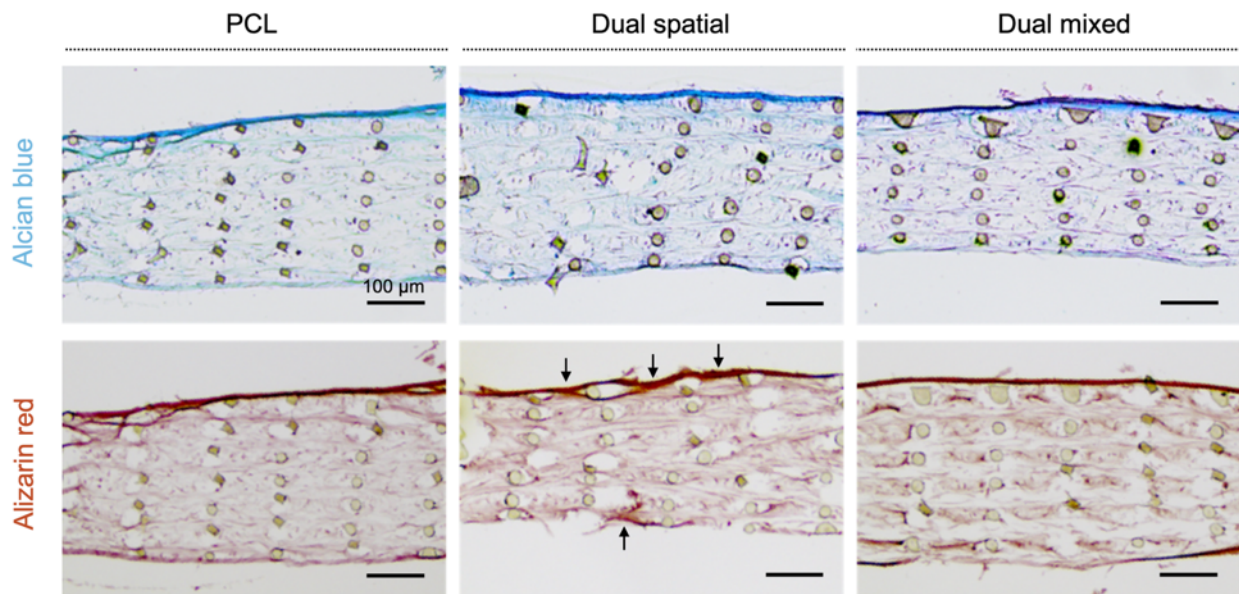


Figure S17. Representative microscopy images of histological cross-sections showing Alcian blue (top) and Alizarin Red (bottom) staining in PCL, dual spatial, and dual mixed scaffolds (L to R). All scaffolds showed similar GAG accumulation. Dual spatial scaffolds showed calcium deposits stained with intense orange-red color (arrows), which was not observed in PCL or dual mixed scaffolds. (Scale bar = 100 μm)

References

- (1) Chow, L. W. Electrospinning Functionalized Polymers for Use as Tissue Engineering Scaffolds. In *Biomaterials for Tissue Engineering. Methods in Molecular Biology*, vol 1758; Chawla, K., Ed.; Humana Press, New York, NY, 2018; pp 27–39. https://doi.org/10.1007/978-1-4939-7741-3_3.
- (2) Camacho, P.; Busari, H.; Seims, K. B.; Schwarzenberg, P.; Dailey, H. L.; Chow, L. W. 3D Printing with Peptide–Polymer Conjugates for Single-Step Fabrication of Spatially Functionalized Scaffolds. *Biomater. Sci.* **2019**, 7 (10), 4237–4247. <https://doi.org/10.1039/C9BM00887J>.
- (3) Chow, L. W.; Armgarth, A.; St-Pierre, J.-P.; Bertazzo, S.; Gentilini, C.; Aurisicchio, C.; McCullen, S. D.; Steele, J. A. M.; Stevens, M. M. Peptide-Directed Spatial Organization of Biomolecules in Dynamic Gradient Scaffolds. *Adv. Healthc. Mater.* **2014**, 3 (9), 1381–1386. <https://doi.org/10.1002/adhm.201400032>.
- (4) Camacho, P.; Fainor, M.; Seims, K. B.; Tolbert, J. W.; Chow, L. W. Fabricating Spatially Functionalized 3D-Printed Scaffolds for Osteochondral Tissue Engineering. *J. Biol.*

Methods **2021**, 8 (1), e146. <https://doi.org/10.14440/jbm.2021.353>.

- (5) Harrison, R. H.; Steele, J. A. M.; Chapman, R.; Gormley, A. J.; Chow, L. W.; Mahat, M. M.; Podhorska, L.; Palgrave, R. G.; Payne, D. J.; Hettiaratchy, S. P.; et al. Modular and Versatile Spatial Functionalization of Tissue Engineering Scaffolds through Fiber-Initiated Controlled Radical Polymerization. *Adv. Funct. Mater.* **2015**, 25 (36), 5748–5757. <https://doi.org/10.1002/adfm.201501277>.